Marine Biotechnology (2024) 26:389–403
https://doi.org/10.1007/s10126-024-10304-0

Comprehensive Multi-omics Approaches Provide Insights to Summer Mortality in the Clam *Meretrix petechialis*

Jing Tian[1,4] · Hongxia Wang[1,2] · Pin Huan[1,2,3] · Xin Yue[1,2] · Baozhong Liu[1,2,3,4]

Received: 16 October 2023 / Accepted: 6 March 2024 / Published online: 14 March 2024

Abstract

Bivalve mass mortalities have been reported worldwide, which not only can be explained as a result of pathogen infection, but may reflect changes in environments. Although these episodes were often reported, there was limited information concerning the molecular responses to various stressors leading to summer mortality. In the present work, RNA sequencing (RNA-seq), tandem mass tagging (TMT)-based quantitative proteomics, and 16S rRNA sequencing were used to explore the natural outbreak of summer mortality in the clam *Meretrix petechialis*. We identified a total of 172 differentially expressed genes (DEGs) and 222 differentially expressed proteins (DEPs) in the diseased group compared to the normal group. The inconsistent expression profiles of immune DEGs/DEPs may be due to the immune dysregulation of the diseased clams. Notably, 11 solute carrier family genes were found among the top 20 down-regulated genes in the diseased group, indicating that weakened transmembrane transport ability might occur in the diseased clams. Integration analysis of transcriptomic and proteomic results showed that many metabolic processes such as "arginine and proline metabolism" and "tyrosine metabolism" were inhibited in the diseased group, suggesting metabolic inhibition. Moreover, 16S rRNA sequencing revealed that the microbial composition of clam hepatopancreas was disordered in the diseased group. The comparison of DEGs expression between the natural summer mortality event and an artificial challenge experiment involving both *Vibrio* infection and heat stress revealed 9/15 genes showing similar expression trends between the two conditions, suggesting that the summer mortality might be caused by a combination of high temperature and *Vibrio* infection. These results would deepen our understanding of summer mortality and provide candidate resistance markers for clam resistance breeding.

Keywords Summer mortality · Multi-omics analysis · *Vibrio parahaemolyticus* · High temperature · *Meretrix petechialis*

Introduction

Marine bivalves are widely distributed from intertidal zones to deep sea and are the essential parts of the marine ecosystem. They perform important ecological functions, not only in food webs but also acting as the sentinels of environmental changes (Vaughn and Hoellein 2018). Many bivalves are vital fishery and aquaculture species that bring significant social and economic benefits to coastal communities. On the other hand, the bivalve culture is threatened by diseases. Mass mortality events are routinely reported worldwide, including those of oysters (Hine et al. 1992; Solomieu et al. 2015), clams (Burdon et al. 2014; Villalba et al. 1999), scallops (Xiao et al. 2005), and mussels (Soon et al. 2016). In general, the mass mortality of bivalves may be attributed to internal (varied genetic backgrounds of hosts) and external factors (pathogens and high temperatures, oxygen depletion, toxic pollutants, etc.) (Alfaro et al. 2019; Burdon et al. 2014; Degremont et al. 2007; Soon and Ransangan 2019). In particular, it is believed that although infectious diseases appear as the main cause of mass mortality, environmental stresses may play a non-negligible role, as they affect both the host/pathogen themselves and their interactions (Barbosa Solomieu et al. 2015; Travers et al. 2015). For instance, high temperatures are believed to be one major cause of bivalve mass mortality (Soon and Zheng 2020). They could lead to mass mortalities by inducing physiological stress of bivalves, or by promoting the proliferation and spread of pathogens (Monari et al. 2007; Ortega et al. 2016; Talmage and Gobler 2011; Tan and Ransangan 2015; Zannella et al. 2017). Studies indeed found that some *Vibrio* diseases often broke out in summer, suggesting a link between high temperatures and disease outbreak (Solomieu et al. 2015).

Extended author information available on the last page of the article

Since the mass mortality of Pacific oyster was reported in 1945, considerable studies have been reported from other bivalves, and the driving factors are investigated. These include the isolation and identification of pathogens from diseased bivalves (Le Roux et al. 2002; Segarra et al. 2010; Yang et al. 2021; Yue et al. 2010), the determination of host risk factors and environmental conditions (Burdon et al. 2014; Solomieu et al. 2015), and selective breeding for resistant strains (Liang et al. 2017). For example, several *Vibrio* species (*V. splendidus* and *V. harveyi*) and OsHV-1 have been detected and suggested to be the major contributors of disease outbreak in certain bivalve species (Alfaro et al. 2019). Li et al. (2020) revealed the metabolic perturbations and protein structural changes in the gill tissues of mussel suffered summer mortality using integrative omics. Despite these notions, however, the knowledge about the biological processes during summer mortality is still limited, especially with regard to the host–pathogen interactions and host response at the molecular level.

We have long worked on infectious diseases in the clam *M. petechialis*, one of the important commercial bivalves distributed in the coastal areas of South and Southeast Asia (Liu et al. 2006). Yue et al. (2010) isolated and identified *Vibrio parahaemolyticus* (MM21) from diseased clams, suggesting that it is the pathogen responsible for the mass mortalities of *M. petechialis* in China. Many infection experiments in the laboratory also confirmed the virulence of pathogen. Several molecular markers associated with *Vibrio* resistance have been identified in our previous works (Nie et al. 2015; Zhang et al. 2017; Zou and Liu 2016). Moreover, we have bred new *Vibrio*-resistant strains of *M. petechialis*, which showed greatly reduced mortality compared to control strains.

In the summer of 2021 (July), we observed a disease outbreak event of *M. petechialis*. The clams of a pond remained generally healthy in the term of 8-month culture from autumn to the next spring. However, under the high temperatures in summer, they suffered a mass mortality in a few days. Interestingly, the clams in the adjacent pond remained healthy during the period, which can be used as an ideal control for investigating the biological changes during summer mortality. In the present study, we used multi-omics approaches to analyze the differences in the transcriptomes, proteomes, and microbiomes of the two batches of clams. The objective of the present work was to explore factors contributing to the summer mortality and molecules that may be involved in the response/adaptation to stressors leading to mass mortality. These results would contribute to a better understanding of summer mortality as well as the molecular basis of resistance traits in bivalves.

Materials and Methods

Experimental Clams and Tissue Collection

The clams used in this work were 42.51 ± 1.88 mm in shell length on average, which were cultured in two adjacent ponds (about 150 clams per square meter) in Wenzhou, China. In July 2021, the water temperature in the pond reached approximately 30 °C; we observed a mass mortality event in one pond, with most clams crawling out of the mud and showing flabby adductor muscle with low responsive activities, most of which died in subsequent few days. This situation, however, was not observed for the adjacent pond, whose clams remained healthy. These two ponds showing varied behaviors were mentioned as "the diseased group" and "the normal group" in the subsequent text.

Twenty clams were randomly selected from each pond for subsequent analyses at the time of disease outbreak. The gill was dissected and equally divided into three parts, each of which was used in transcriptomic, proteomic, or 16S rRNA sequencing analysis. The hepatopancreas was also sampled and used for 16S rRNA sequencing analysis. In these assays, the same tissue of four clams was mixed as one replicate, i.e., there had a total of five biological replicates per group. The samples were quickly frozen in liquid nitrogen and stored at − 80 °C before using.

Transcriptome Sampling, Sequencing, and Bioinformatics Analysis

Total RNA was extracted from the gill tissue using Trizol reagent according to the manufacturer's instructions (Invitrogen, USA). The concentration and purity of the extracted RNA were assessed using an Agilent 2100 bioanalyzer. Sequencing libraries were constructed using the NebNext®Ultra™ RNALibrary Prep Kit for Illumina® (NEB, USA). After evaluation of the library quality, sequencing was performed using Illumina HiSeq platform for 150 bp paired-end reads. The transcriptome sequencing libraries in the diseased and normal group produced a total of 110,608,112 and 109,764,695 raw reads, respectively.

Clean data were obtained after quality control and filtration by removing low-quality reads. Similar numbers of clean reads (107,910,862 and 105,710,984 clean reads, respectively) were generated after quality control and data filtering (Supplementary Table 1). Trinity (Grabherr et al. 2011) was used to assemble clean reads to obtain reference sequences for subsequent analysis. Gene function was annotated based on the following databases: Nr, Nt, Pfam, KOG/COG, Swiss-Prot, KO, and GO. DESeq R package (1.10.1) was used to identify the differential expression genes (DEGs) between two groups following a threshold (P-adjust < 0.05 and $|\log_2$ Foldchange$| \geq 1$). The GO and

KEGG pathway enrichment analysis of DEGs was further carried out using Goseq and KOBAS software (Young et al. 2010). Principal component analysis (PCA) was performed on gene expression values (fragments per kilobase of exon per million mapped reads, FPKM) of all samples.

Protein Extraction, Sequencing, and Analysis

Protein lysate was added to the gill on ice for 5-min ultrasonication. The supernatant was collected after centrifugation (12,000 *g*, 4 °C, 15 min). Dithiothreitol and iodoacetamide were then added in the dark at room temperature. Precooled acetone was added to precipitate at − 20 °C for at least 2 h, centrifuged at 4 °C at 12,000 *g* for 15 min, and the precipitation was collected and air dried. Finally, the protein solution is added (6 M urea, 100 mM triethylammonium bicarbonate (TEAB), pH = 8.5) to dissolve protein precipitates. The protein concentration was assessed using a Bradford Protein Assay kit following the instruction from the manufacturers.

The protein (120 μg) was labeled according to the manufacturer's protocol for TMT® Mass Tagging Kits and Reagents (Thermo, USA). Trypsin (Promega, USA) was added to the protein sample and digested overnight at 37 °C. The tryptic-digested peptides were desalted and vacuum freeze-dried, and the peptides were solubilized with TEAB (Sigma, USA). Labeled peptides were fractionated by reversed phase chromatography, which was performed by L-3000 HPLC (RIGOL Technologies, China) using a Waters BEH C18 column (4.6 × 250 mm, 5 μm). The eluates were monitored under UV 214 nm, with one tube collected per minute and finally pooled into 10 fractions. All fractions were dried under vacuum and then reconstituted in 0.1% (v/v) formic acid in water. The separated peptides were analyzed by Q Exactive HF-X mass spectrometer (Thermo Fisher, USA) with ion source of Nanospray Flex™ (ESI). For MS analysis, we applied the data-dependent acquisition mode. The range of full scan MS spectra was set from 350 to 1500 m/z with a resolution of 60,000 (at m/z 200). For MS/MS analysis, the higher energy collisional dissociation fragmentation was carried out with the resolution at 45,000 (at m/z 200) for 10 plex.

The raw data were searched against the *M. petechialis* transcriptome database using the Proteome Discoverer software (PD 2.2, Thermo). To reduce the probability of identifying incorrect peptides, the results were further filtered to remove peptides and proteins with false discovery rate (FDR) greater than 1%. The threshold (fold change (FC) ≥ 1.20 or FC ≤ 0.83) of differentially expressed proteins (DEPs) between two groups was set at *P* value lower than 0.05. Functional classification of DEPs was conducted via GO enrichment and pathway enrichment analysis. PCA analysis was kept in line with the transcriptome as mentioned above.

Combined Challenges Experiment and Quantitative Real-Time PCR Analysis

To compare the gene expression between the samples suffering summer mortality and artificial infection, combined challenges was performed according to Zhang et al. (2019). A concentration of 1×10^7 CFU ml^{-1} of *V. parahaemolyticus* was used, and the clams were cultured at 31 ℃. Gills were dissected from the clams sampled at 0 and 5 dpi (days post-infection), and total RNA was extracted using SPARKeasy Improved Tissue/Cell RNA Kit (SparkJade, China) following the manufacturer's protocol. The extracted RNA was quantified using a Nanodrop ND1000 spectrophotometer (Thermo Scientific, USA) and assessed using agarose gel electrophoresis. First-strand cDNA synthesis was performed using HiScript III 1st Strand cDNA Synthesis Kit (Vazyme, China).

The top 15 down-regulated DEGs revealed by transcriptomic analysis on the diseased group in the mortality event, which included 10 solute carrier family genes (SLCs; see details in the "Results" section), were used for qPCR analysis. The primers used for qPCR were provided in Supplementary Table 2 and the elongation factor 1 alpha gene (EF1α) was chosen as the internal reference to normalize the relative expression levels (Fabioux et al. 2004; Jiang et al. 2017; Tian et al. 2021). The qPCR was performed using a Bio Rad CFX 96 Real-time PCR system using SYBR premix (TaKaRa, Japan). The PCR program was set as 95 °C for 30 s, 40 cycles of 95 °C for 5 s, and 60 °C for 30 s, followed by melting curve analysis. The relative expression level of genes was analyzed using the $2^{-\Delta\Delta CT}$ method (Livak and Schmittgen 2001).

Bacterial Microbiota Analysis

To better understand the microbiota changes in the host, 16S rRNA sequencing was performed using gill and hepatopancreas. Detailed information about the procedure was described in our previous study (Wang et al. 2020). Briefly, total genome DNA from gill and hepatopancreas was extracted using the CTAB/SDS method. The V4-V5 region of 16S rRNA gene was amplified using a specific primer (515F-806R) containing different barcodes. Sequencing libraries were generated using a TruSeq® DNA PCR-Free Sample Preparation Kit (Illumina, USA) following the manufacturer's instructions. Sequencing was performed using an Illumina NovaSeq platform for 250 bp paired-end reads.

The raw data was spliced and filtered to obtain clean data, and then paired-end reads were merged using FLASH (Magoc and Salzberg 2011). Operational taxonomic units (OTUs) were clustered with an equivalence of 97% using UPARSE (Edgar 2013). Rarefaction curve was analyzed by R package, which can reflect the rationality of sequencing

data and the richness of species in samples. Principal coordinate analysis (PCoA) was performed by the WGCNA package, stat packages, and ggplot2 package in R software. MRPP (Multi-Response Permutation Procedure) analysis was obtained using MRPP function of R package.

Results

Characterization of Transcriptomic and Proteomic Data and PCA Analysis

A total of 178,299 unigenes with an N50 length of 924 bp were assembled, derived from 509,979 high-quality transcripts generated during RNA-seq (Supplementary Table 1). In proteomic analysis, a total of 412,691 spectra was obtained after LC/MC analysis, producing 11,245 proteins identified from 72,941 peptides with a criterion of FDR below 1% and confidence interval of 99%.

PCA analysis was performed among the 10 samples from diseased and normal groups based on the transcriptomic or proteomic data (Fig. 1). At the transcriptional level, the diseased samples were clustered together tightly and all were within the 95% confidence interval, while the distribution of normal samples was relatively scattered (Fig. 1A). The difference between the diseased group and the normal group was more obvious at the protein level, which was distinguished on the first principal component with a contribution value of 16.8% (Fig. 1B). These results indicated that the normal and diseased groups produced considerable differences at both the transcriptional and protein levels.

Transcriptomic Changes in the Diseased Clams

In transcriptomic analysis, a total of 172 DEGs were identified between the gill tissues of the two groups. Compared with the normal group, there were 108 down-regulated DEGs and 64 up-regulated DEGs in the diseased group. Figure 2 shows the volcano plots and heat map of the overall distribution of DEGs. The top 20 up-regulated and down-regulated genes are listed in Table 1. Some immune-related genes (E3 ubiquitin–protein ligase RNF 213-alpha-like, sialic acid–binding lectin, and interferon-induced protein 44-like) and inflammation-related gene (angiopoietin-related protein 2-like) showed significantly different expression profiles in the diseased group, indicating that the immune system of the clams was activated. Notably, almost all top 20 down-regulated genes were related to transporters, in which SLCs accounted for 11/20. In particular, they accounted for 10 of the top 15 down-regulated genes. The down-regulation of SLCs in the diseased group suggested that the transmembrane transport ability of the diseased individuals was impaired, which is essential to understand the disease process of clams.

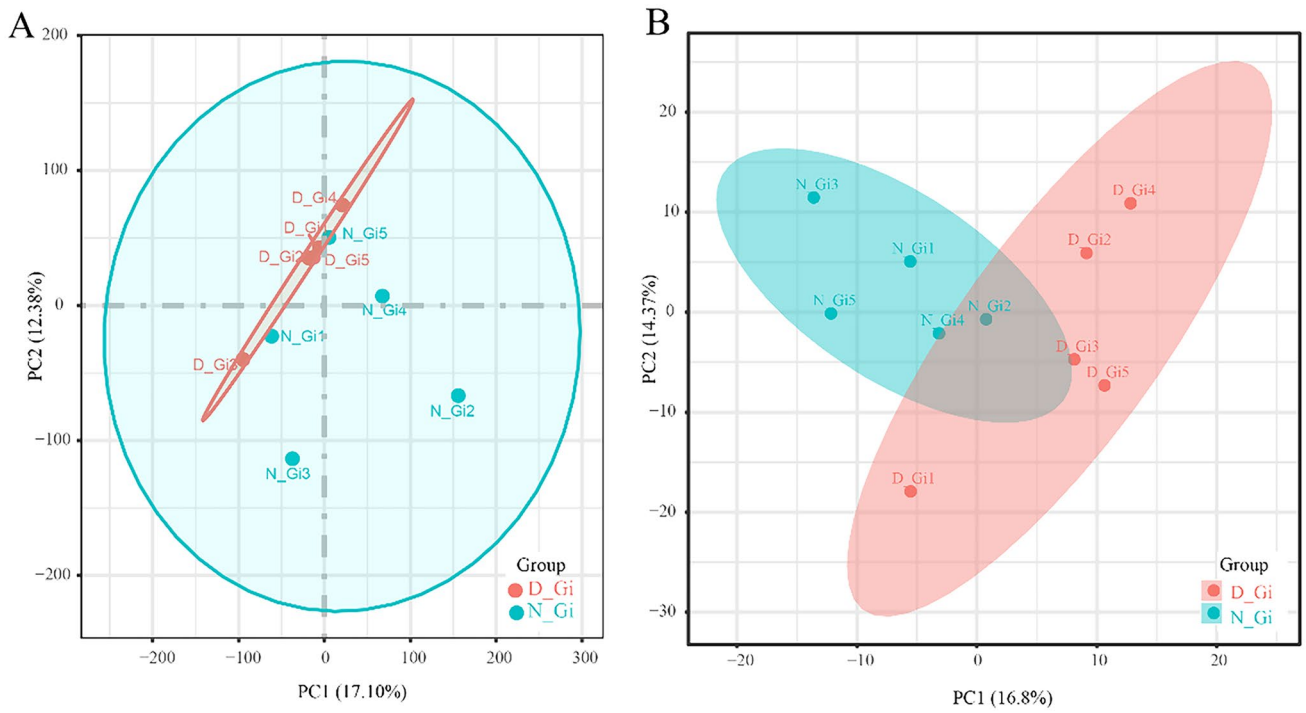

Fig. 1 Principal component analysis (PCA) of transcriptome (**A**) and proteome (**B**). Each point corresponds to one replicate of four clams. Diseased gill and normal gill are abbreviated as D_Gi and N_Gi

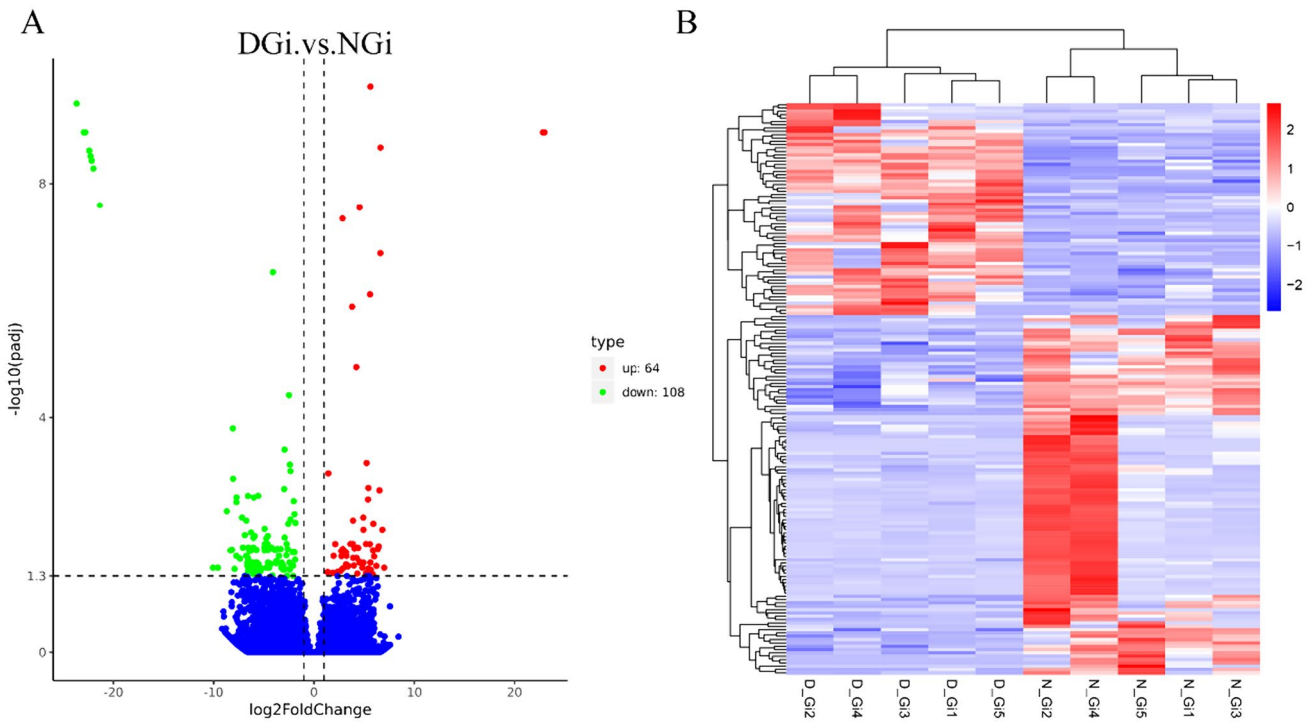

Fig. 2 Transcriptomic profiling reveals altered gene transcription patterns in *M. petechialis*. **A** Volcano plots showing differentially expressed genes (DEGs) identified between the two groups. Dots highlighted in red and green indicate up-regulated genes and down-regulated genes (*P*-adjust < 0.05). **B** Heat map of DEGs in diseased group compared with the control. The rows represent individual genes. Different colors represent different relative abundance of genes, where red represents higher intensity and blue represents lower intensity. Diseased gill and normal gill are abbreviated as D_Gi and N_Gi

GO analysis and KEGG analysis were further conducted to understand the biological significance of DEGs between the two groups. As shown in Fig. 3A, "localization" and "transmembrane transport" were the most down-regulated enriched items in the category of biological process. The top 20 significant pathways were shown in Fig. 3B. The results showed that six metabolic pathways were significantly down-regulated in the diseased groups, which contained "Choline metabolism in cancer," "Vitamin digestion and absorption," "Retinol metabolism," "Fructose and mannose metabolism," "Alanine, aspartate and glutamate metabolism," and "Glycine, serine and threonine metabolism," indicating that the diseased group may be related to metabolic depression ($P < 0.05$).

Identification of Differential Expression Proteins and Functional Annotation

TMT and LC–MS/MS analysis of the gill revealed 222 DEPs, including 65 up-regulated proteins and 157 down-regulated proteins compared with the normal group. As shown in Fig. 4, these DEPs displayed distinct profiles between the two groups. The details of top 20 up-regulated and down-regulated DEPs are summarized in Table 2. Similar to the transcriptomic results, more down-regulated proteins were identified than up-regulated proteins in proteome. Several immune-related DEPs involved in recognition terms (C1q-like protein 4), immune signaling mediators (E3 ubiquitin-protein ligase RNF213), effector protein (TGTP1-like), and inflammatory response protein (low-density lipoprotein receptor–related protein 6, ldlr6) were down-regulated in the diseased group.

The biological processes among DEPs were revealed with enrichment analysis. In the terms of biological process, four DEPs were founded to be associated with cell adhesion (Fig. 5A), which were probably linked to host defense against pathogen colonization in vivo. Consistently, adhesions junction was the most enriched pathway in KEGG analysis (Fig. 5B). Moreover, similar to transcriptomic results, KEGG analysis also enriched five down-regulated metabolic pathways, which further implies that the proper functioning of substance metabolism is critical to the clam's health.

Table 1 The top 20 up-regulated and down-regulated differentially expressed genes

Gene ID	DEG name	log_2FC
Cluster-8621.11396	SVEP1	22.227
Cluster-8621.76083	Contactin	6.4628
Cluster-8621.80813	Hus1-like	5.9938
Cluster-8621.70584	Axoneme-associated protein	5.9203
Cluster-8621.96498	Heavy metal-binding protein HIP-like	5.6945
Cluster-8621.123661	E3 ubiquitin-protein ligase RNF213-alpha-like	5.6281
Cluster-8621.52887	sialic acid-binding lectin	5.5867
Cluster-8621.66116	Phenazine biosynthesis protein A/B	5.5680
Cluster-8621.43537	Angiopoietin-related protein 2-like	5.4285
Cluster-8621.126142	PERQ amino acid-rich with GYF domain-containing protein 2-like	5.3861
Cluster-8621.129301	SVEP1-like	4.9322
Cluster-27530.1	Potassium voltage-gated channel protein egl-36	4.8246
Cluster-8621.61449	Hypothetical protein BRAFLDRAFT	4.2700
Cluster-8621.96111	DNA polymerase eta-like	4.2359
Cluster-8621.52888	Heavy metal-binding protein HIP-like	4.2211
Cluster-8621.130824	Hypothetical protein AC249_AIPGENE22917	3.9057
Cluster-8621.47847	E3 ubiquitin-protein ligase TRIM71	3.8795
Cluster-8621.43515	Poly [ADP-ribose] polymerase 14-like	3.2445
Cluster-8621.60140	G-Protein coupled receptor 153	2.8867
Cluster-8621.14815	Interferon-induced protein 44-like	2.1193
Cluster-8621.23300	Cytochrome P450 1A1-like (CYP1A1)	− 23.547
Cluster-8621.134160	Sodium-coupled monocarboxylate transporter 1-like (SLC5A8_1)	− 23.019
Cluster-8621.29367	Monocarboxylate transporter 6-like (SLC16A6)	− 8.3190
Cluster-8621.2436	Solute carrier family 23 member 1-like (SLC23A1)	− 8.0628
Cluster-8621.2659	Excitatory amino acid transporter 1-like (SLC1A3)	− 7.9181
Cluster-8621.134157	Solute carrier family 22 member 8-like (SLC22A4_5_1)	− 7.7471
Cluster-8621.29366	Monocarboxylate transporter 14 (SLC16A14)	− 7.7338
Cluster-8621.133906	Solute carrier family 22 member 4-like (SLC22A4_5_2)	− 7.7248
Cluster-8621.2658	Multidrug resistance-associated protein 1-like (ABCC1)	− 7.1772
Cluster-8621.2684	Sodium-coupled monocarboxylate transporter 1-like (SLC5A8_2)	− 7.0815
Cluster-8621.132518	Zinc transporter ZIP14-like (SLC39A14, ZIP14)	− 6.7481
Cluster-8621.32466	Trace amine-associated receptor 1 (TAAR1)	− 6.7427
Cluster-8621.5517	Monocarboxylate transporter 12-like (SLC16A12)	− 6.6435
Cluster-8621.40066	Cadherin-23-like (FAT4)	− 6.6343
Cluster-8621.26880	Mitochondrial enolase superfamily member 1-like (FucD)	− 6.5992
Cluster-8621.37115	Sodium and chloride-dependent glycine transporter 2 (SLC6A5S)	− 6.5849
Cluster-8621.76460	AB hydrolase superfamily protein C1039.03	− 6.5396
Cluster-8621.2059	Peptidase M20 domain-containing protein 2-like	− 6.5316
Cluster-8621.97651	Octopine dehydrogenase (OcDH)	− 6.5287
Cluster-8621.63608	Serine-pyruvate aminotransferase (AGXT)	− 6.2716

Integration of the Transcriptome and Proteome

The integration of the transcriptomic and proteomic data was performed to illustrate the correlation of expression at gene and protein levels between the normal and diseased group. GO correlation analysis showed that "metabolic processes," "cellular processes," and "responses to stimuli" were well correlated in biological process, and for molecular functions, "catalytic activity," "binding," and "antioxidant activity" had a good correlation (Fig. 6A). KEGG enrichment association analysis revealed that there were four clustering types according to the protein/gene expression patterns enriched into each horizontal item. Both "Arginine and proline metabolism" and "Tyrosine

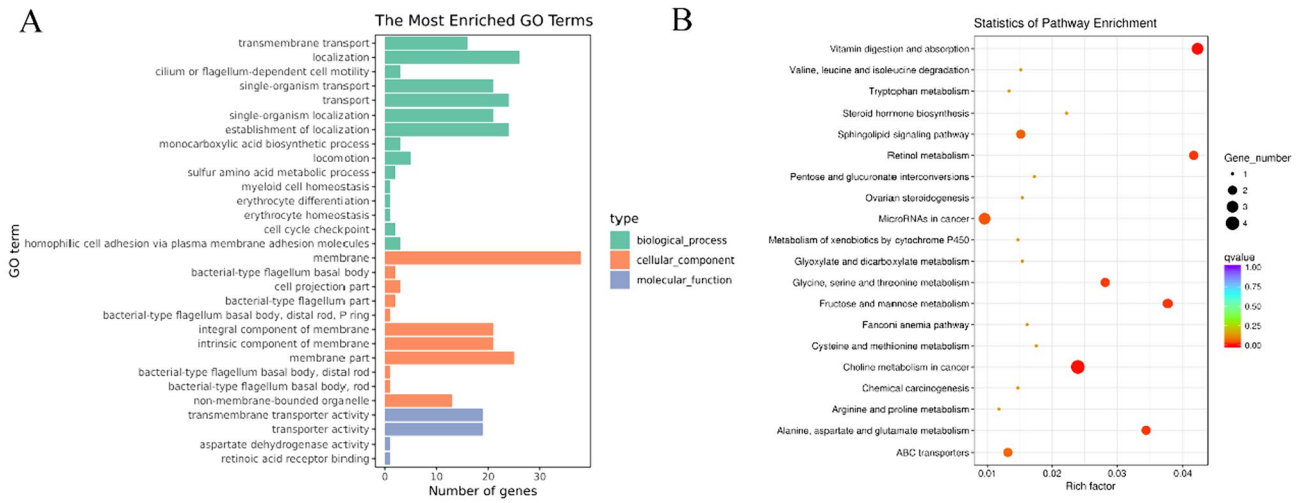

Fig. 3 Functional classification for all DEGs. **A** GO enrichment analysis histogram. The DEGs were classified into three functional categories, biological process (BP), cellular component (CC), and molecular function (MF). If there are less than 30 terms, draw all terms, as shown in the figure below. The horizontal axis represents the number of DEGs; the vertical axis represents GO terms. **B** KEGG pathway enrichment analysis of differentially expressed genes

metabolism" were down-regulated in transcriptomes and proteomes (Fig. 6B). Additionally, a total of three proteins exhibited similarly down-regulated expression profiles as their corresponding encoding genes, including sarcoplasmic calcium binding protein (SCP), CYP4B1, and DUR3-like urea-proton symporter (Fig. 6C). These results showed that although only a few shared genes (proteins) were identified, the association at a broader functional class showed good consistency between the transcriptional and protein level.

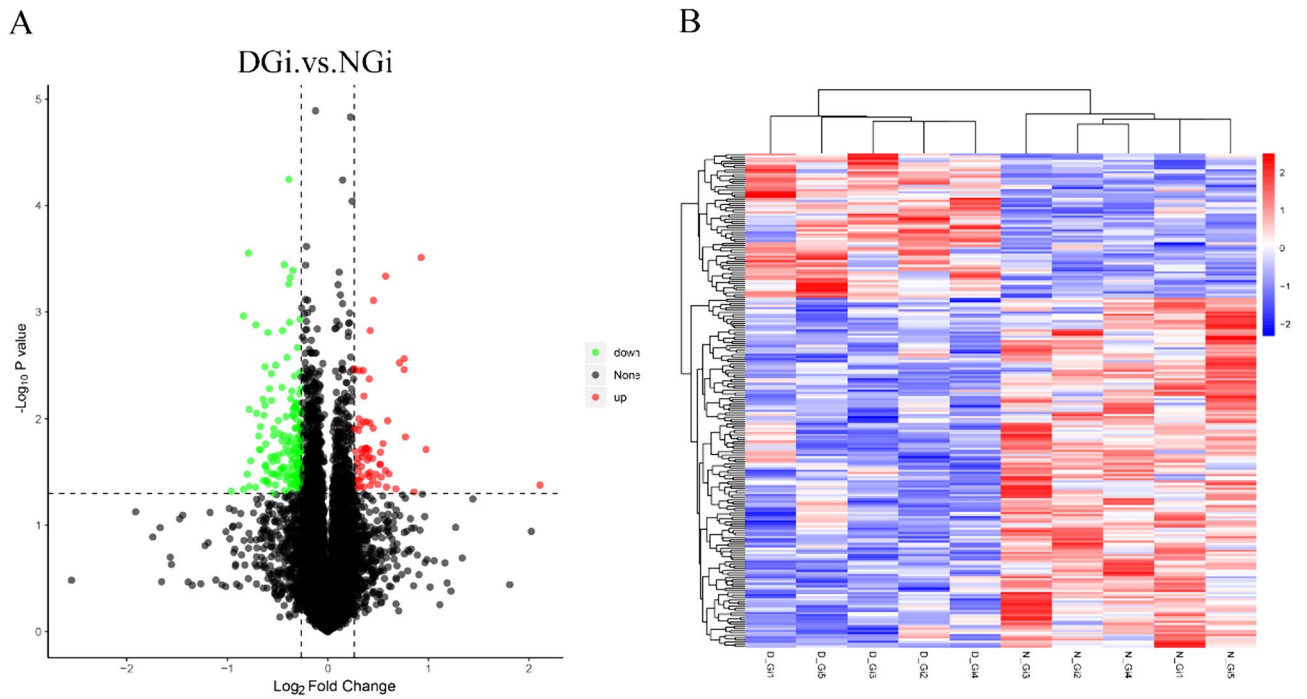

Fig. 4 Proteomic profiling reveals altered protein expression patterns. **A** Volcano plots showing differentially expressed proteins (DEPs) identified between the two groups. **B** Heat map of DEPs in diseased group compared with the normal group. Diseased gill and normal gill are abbreviated as D_Gi and N_Gi

Table 2 The top 20 up-regulated and down-regulated differentially expressed proteins

Protein ID	DEP name	log_2FC
Cluster-8621.124475; orf1	NFX1-type zinc finger-containing protein 1-like	0.9776
Cluster-8621.106951; orf1	SVEP1-like	0.9279
Cluster-8621.7318; orf1	Excitatory amino acid transporter 1-like	0.7585
Cluster-8621.70414; orf1	E3 ubiquitin-protein ligase TRIM56	0.7131
Cluster-15043.0; orf1	Protocadherin Fat 4-like	0.6760
Cluster-8621.79996; orf1	Hypoxia-inducible factor 1-alpha	0.6071
Cluster-8621.78647; orf2	E3 ubiquitin-protein ligase rnf213-alpha-like,	0.5726
Cluster-8621.129326; orf1	Alkaline phosphatase, tissue-nonspecific isozyme-like	0.5482
Cluster-8621.53717; orf2	E3 ubiquitin-protein ligase MIB1	0.5234
Cluster-8621.72665; orf1	Peptidoglycan recognition protein short	0.5166
Cluster-8621.57830; orf1	Vitelline membrane outer layer protein 1	0.4769
Cluster-8621.26217; orf1	Annexin A7-like	0.4537
Cluster-8621.45365; orf1	Neurocalcin	0.4475
Cluster-8621.114041; orf1	Wiskott-Aldrich syndrome protein	0.4208
Cluster-8621.90293; orf1	Cathepsin L	0.4098
Cluster-8621.45360; orf1	Seminal fluid protein	0.3953
Cluster-23777.0; orf1	SVEP1-like	0.3848
Cluster-8621.69673; orf1	2-Oxo-4-hydroxy-4-carboxy-5-ureidoimidazolinedecarboxylase-like	0.3403
Cluster-8621.129361; orf1	NACHT domain- and WD repeat-containing protein 1-like	0.3363
Cluster-8621.25255; orf1	DNA-directed RNA polymerase I subunit RPA2	0.3343
Cluster-8621.78526; orf1	4-Coumarate-CoA ligase 4-like	−0.9605
Cluster-8621.80976; orf1	DUR3-like urea-proton symporter	−0.8025
Cluster-8621.62601; orf1	Nephrin-like	−0.7825
Cluster-8621.129356; orf1	Sulfotransferase family cytosolic 1B member 1-like	−0.7667
Cluster-8621.39894; orf2	Cytochrome P450 4A25	−0.7182
Cluster-8621.134691; orf1	T-Cell-specific guanine nucleotide triphosphate-binding protein 1-like	−0.7155
Cluster-8621.16931; orf1	low-density lipoprotein receptor-related protein 6	−0.6810
Cluster-8621.53992; orf1	T-Cell-specific guanine nucleotide triphosphate-binding protein 1-like	−0.6248
Cluster-8621.100460; orf1	Protein FORGETTER 1-like	−0.6204
Cluster-8621.99691; orf1	DBH-like monooxygenase protein 1	−0.6203
Cluster-8621.99691; orf2	DBH-like monooxygenase protein 1	−0.6180
Cluster-8621.125888; orf1	Complement C1q-like protein 4	−0.5968
Cluster-8621.45399; orf1	E3 ubiquitin-protein ligase rnf213-alpha-like	−0.5910
Cluster-8621.57200; orf1	Fatty acid-binding protein, heart-like	−0.5613
Cluster-8621.54617; orf1	Plasminogen	−0.5591
Cluster-8621.93418; orf2	Dehydrogenase/reductase SDR family member 4-like	−0.5455
Cluster-8621.93418; orf2	Nephrin-like	−0.5407
Cluster-8621.26771; orf1	Heat shock 70 kDa protein 12B-like	−0.5367
Cluster-8621.81052; orf1	Transmembrane protein 177-like	−0.5354
Cluster-8621.68629; orf1	E3 ubiquitin-protein ligase TRIM33-like	−0.5193

Comparison of DEG Expression in Two Diseased Events

Previous studies in our laboratory have shown that high temperatures could exacerbate mortality caused by pathogen challenges (Yue et al. 2018). To explore whether the clams from natural summer mortality experienced a similar biological process with combined challenges of *Vibrio* infection and heat stress, we compared the expression profiles between the natural summer mortality event and an artificial challenge experiment. As aforementioned, transcriptomic analysis on the diseased clams during the mortality event revealed that SLCs accounted for 10 of the top 15 down-regulated genes (Table 1); we thus focused on these 15 genes and explored their expression in the artificially challenged clams via qPCR. As shown in Fig. 7, 9 genes

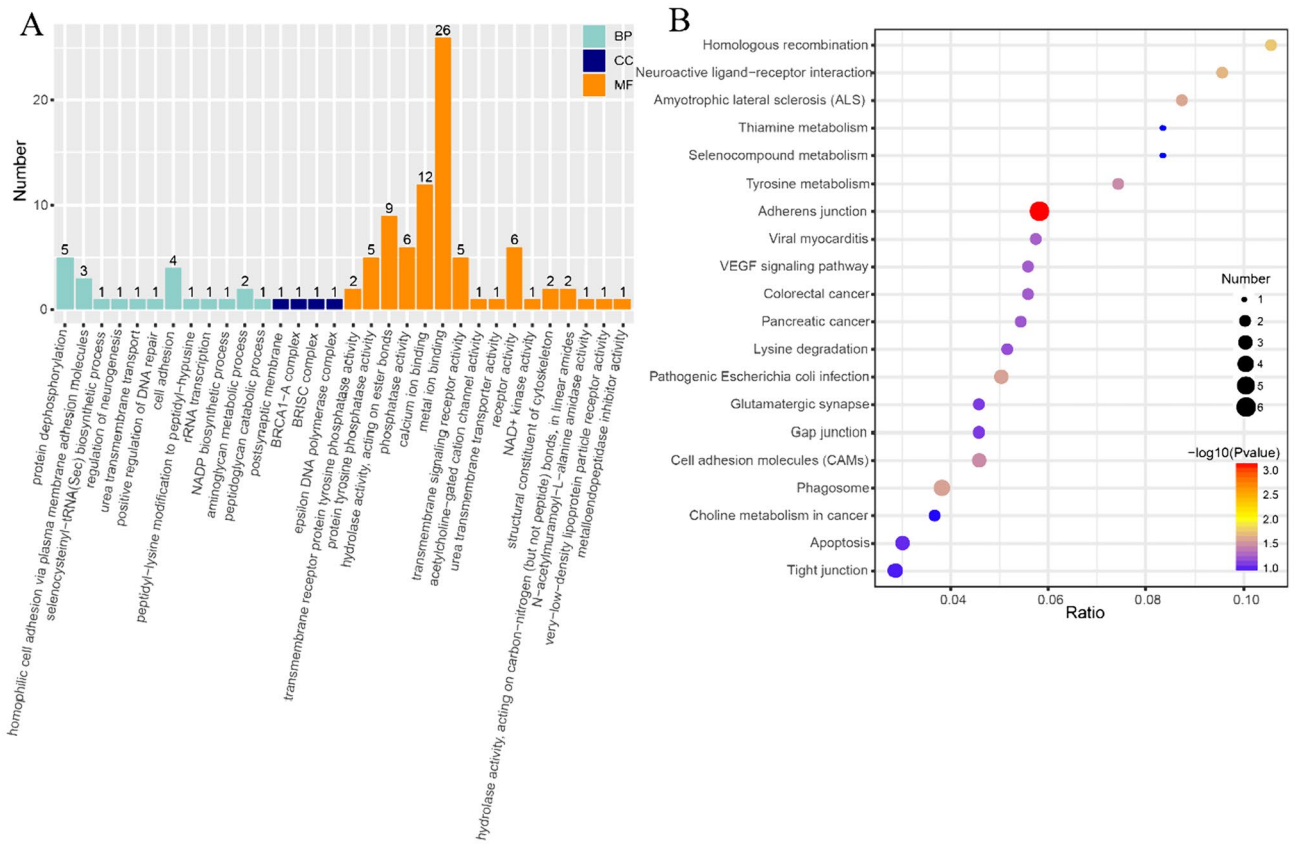

Fig. 5 Functional classification for all DEPs. **A** Enrichment analysis showing the top 30 enriched GO categories in the DEPs. **B** KEGG pathway enrichment analysis of differentially expressed proteins

were significantly down-regulated at 5 dpi after combined challenges compared with control group, meaning that 9/15 genes had similar expression profiles between the two disease events. These results suggested that the clams that suffered summer mortality seem to undergo a similar biological process as the clams with *Vibrio* infection and heat stress.

16S rRNA Sequencing Analysis

To explore the microbiota changes of clams suffering summer mortality, we performed 16S rRNA sequencing analysis on the gill and hepatopancreas since the gill is implicated in filtering the surrounding water (Saco et al. 2020) and the hepatopancreas is the primarily bacterial accumulation tissue within mollusks (Rubiolo et al. 2018). Overall, we obtained 868,545 and 887,787 raw sequencing reads from the hepatopancreas and gill of 10 samples (Supplementary Table 3).

As shown in Fig. 8, there were evident differences in the relative abundance of OTUs in the hepatopancreas between the two groups. *Cyanobacteria* were the dominant species in the normal group, while the composition of microorganisms in the diseased group changed obviously, suggesting that there was a disorder of the microbial community in the diseased groups (Fig. 8A). PCoA analysis showed that the microbial composition of the hepatopancreas between the diseased group and the normal group was separated by the second principal coordinate (20.75%) (Fig. 8B), and results of MRPP parameters based on Bray–Curtis distance also indicated the difference was statistically significant (Supplementary Table 4).

By contrast, the relative abundance of species in gills was very similar between the diseased group and the normal group (Fig. 8A). Principal coordinate analysis (PCoA) based on weighted UniFrac distance also displayed the microbial communities of the gills clustered together, and there was no significant difference between two groups (Fig. 8B).

Discussion

The massive summer mortality of bivalves has been frequently reported around the world, causing enormous losses to aquaculture. It is still difficult to determine the

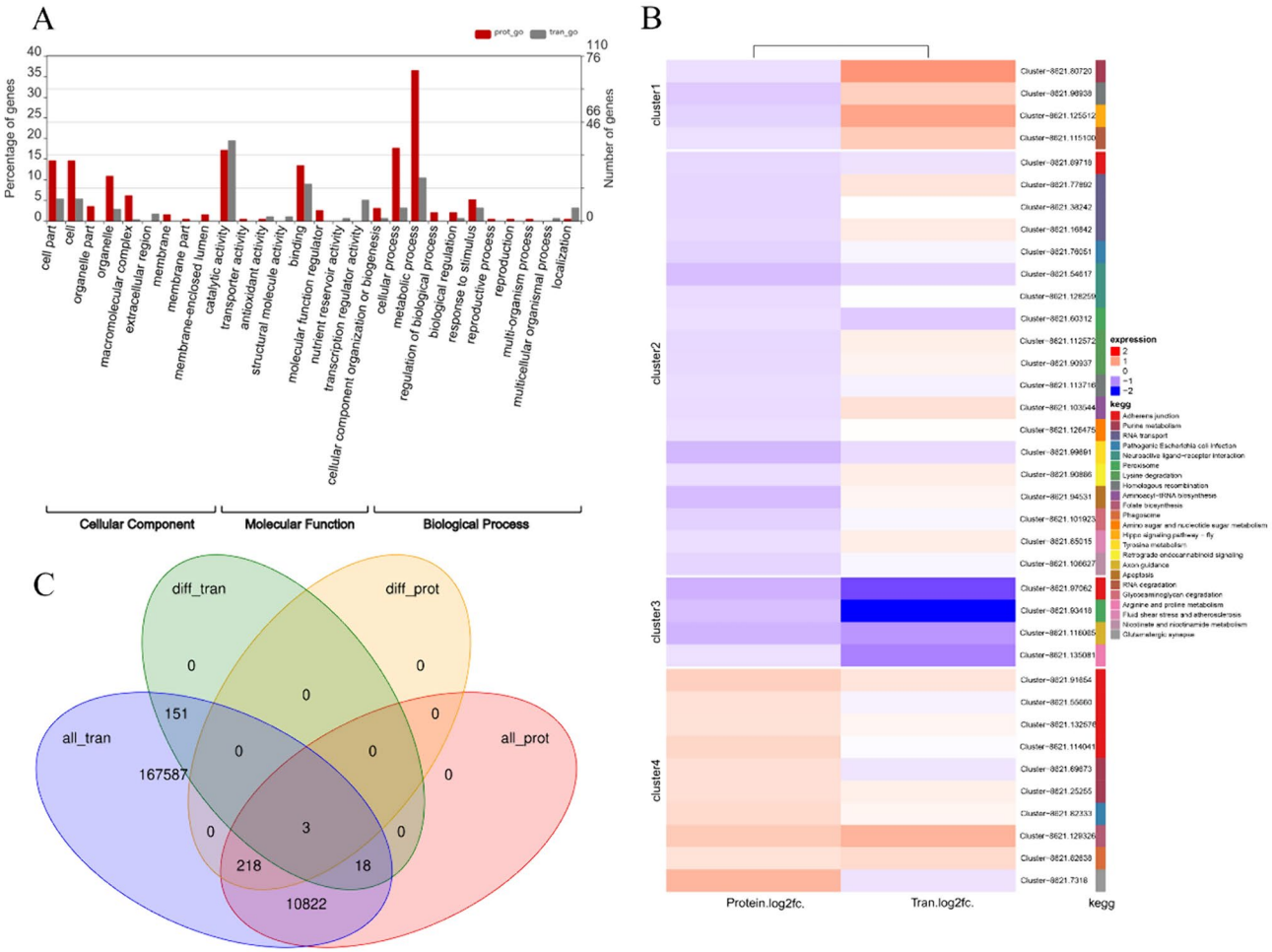

Fig. 6 Correlation analysis of the transcriptome and proteome. **A** Association analysis of GO enrichment based on DEGs/DEPs between DGi and NGi. **B** Association analysis of KEGG pathway based on DEGs/DEPs between DGi and NGi. **C** Venn diagrams of all identified genes, DEGs, all identified proteins, and DEPs

definitive causes of mass mortality events, and interactions between host and pathogen are still not fully understood. This bottleneck for shellfish cultivation requires the application of multiple approaches. Recently, various studies focused on the characterization of host and pathogen genomes, transcriptomic and proteomic responses to pathogens, and effects of pathogens on metabolome (Jiang et al. 2021; Nguyen et al. 2019; Saco et al. 2021). While different approaches focus on different aspects, the integration of these techniques may show unique strengths. Indeed, as we have shown in the present study, integrated omics could provide comprehensive insights into our understanding of mass mortalities.

The clams that suffered mass mortality provide good materials for studying the possible causes of such natural mass mortalities. It has been shown that the causes of summer mortality in bivalves are complex, and pathogen infection is one of the major causes of death in marine mollusks. Several *Vibrio* species are important pathogens that affected mortality outbreaks of cultivated bivalves (oysters, clams, and mussels). Among them, the *Splendidus* clade (e.g., *V. splendidus*, *V. tasmaniensis*, and *V. crassostreae*), the *Harvey* clade, and others (*V. aestuarianus*, *V. tubiashii*, *V. coralliilyticus*, and *V. tapetis*) are often associated with bivalve mortality (Travers et al. 2015). At the same time, it is agreed that environmental factors such as high temperatures appear to be critical driving forces of bivalve mass mortalities (Barbosa Solomieu et al. 2015; Burge et al. 2006; Clegg et al. 2014). To explore the potential driving factors of the mortality of *M. petechialis*, we compared the gene expression between the clams suffering natural summer mortality and those under combined challenges (*Vibrio* infection and heat stress). We found that among 15 down-regulated genes investigated, 9 genes showed similar trends of expression changes by qPCR analysis, accounting for a 60% similarity. These results indicate similar biological processes between

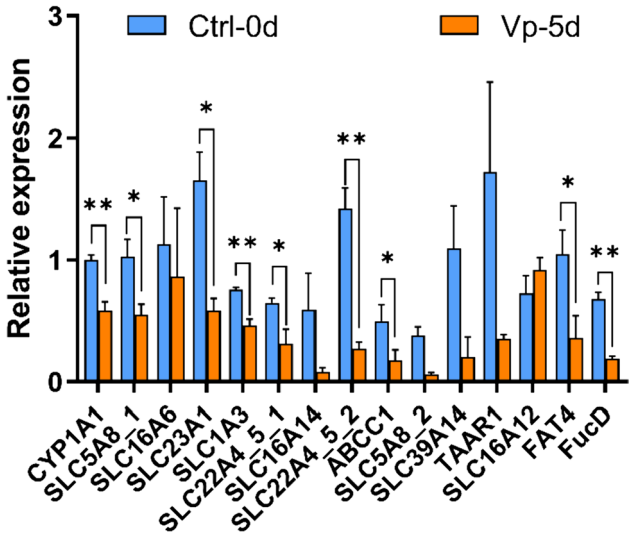

Fig. 7 Relative expression of top 15 down-regulated DEGs. The statistical analysis was performed using a two-tailed *t*-test. Values are shown as mean ± S.E. Significant difference compared to the control expression level was marked with asterisks (*$0.01 < P < 0.05$; **$P < 0.01$)

combined challenges in the laboratory and the natural summer mortality, hinting that the summer mortality may be caused by the combination of vibriosis and heat stress.

Indeed, high temperatures could aggravate *Vibrio* infection. High-temperature–induced bivalve mass mortality may result from energy deficiency, which in turn affects growth, reproduction, and immunity (Ivanina et al. 2013). High temperatures may also promote the proliferation and spread of pathogenic bacteria, increasing host susceptibility to harmful bacteria (Petton et al. 2013; Vezzulli et al., 2010). Besides, numerous previous studies have shown that high temperatures can significantly alter microbial diversity and community dynamics (Go et al. 2017). For example, Li et al. (2018) found that elevated temperatures decreased microbial diversity in *Mytilus coruscus*. The disordered microflora in hepatopancreas of our results may be closely related to the high temperature.

Altered expression patterns of immune-related molecules are a common phenomenon in animals after bacterial infection (He et al. 2022; Saco et al. 2020). According to our results, immune genes such as E3 ubiquitin protein ligase, lectin, and interferon-induced protein 44-like were significantly up-regulated in the diseased group at the transcriptional level, while some immune-related proteins which regulate the phagocytosis (Liang et al. 2019; Lv et al. 2018), such as encoding C1qDC proteins and ldlr6, were inhibited in the diseased group at the protein level (Table 2). The inconsistent expression profiles of immune genes/proteins may be due to the immune dysregulation of the diseased clams. We hypothesized that the up-regulation of immune genes may indicate the active defense to adverse conditions, and the down-regulation of immune genes expression may be related to immunosuppression. Indeed, immunosuppression was revealed in oysters with Pacific oyster mortality syndrome, which leads to the proliferation of bacteria (de Lorgeril et al. 2018). Taken together, our results suggest that the immune system of diseased clams responds to the various stressors during summer mortality, although it requires further investigations to determine whether the changes in immune genes would reflect the host's active antimicrobial defense, immunosuppression, or even the disorders of the host immune system.

In the transcriptomic analysis, we found the expression of a large number of SLC genes was significantly suppressed

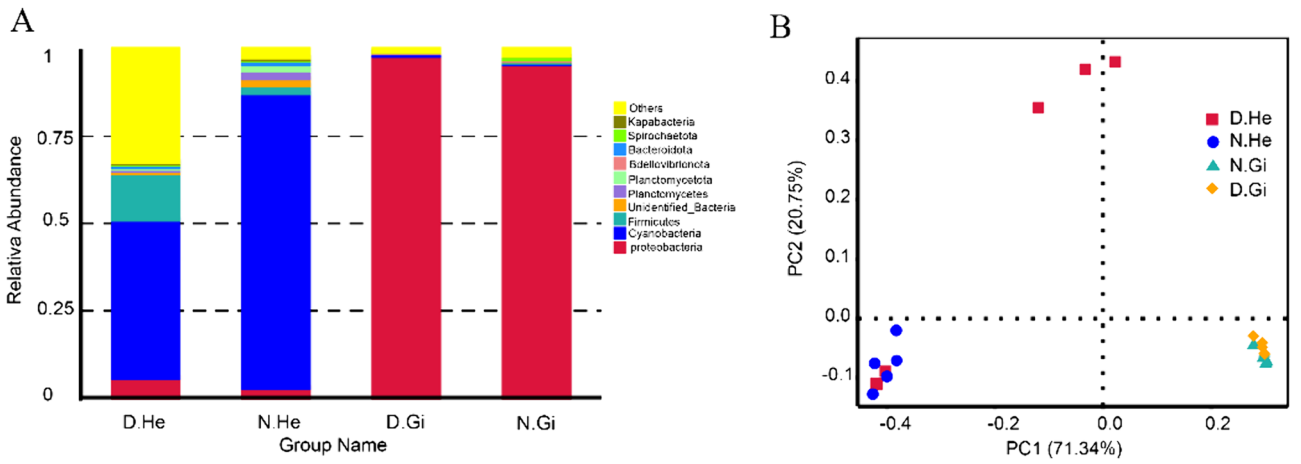

Fig. 8 Microbiota changes in the diseased group and normal group. **A** The histogram of relative abundance of species at the phylum level. The abscissa is the group name; the ordinate represents the relative abundance; others represent the sum of the relative abundances of all other phyla except these 10 phyla in the figure. Diseased gill, normal gill, diseased hepatopancreas, and normal hepatopancreas are abbreviated as D. Gi, N. Gi, D. He, and N. He. **B** Principal coordinate analysis based on weighted UniFrac distance

in the diseased group. Previous studies have shown that the roles of SLC genes may be related to energy balance, oxidative defense, and nervous system homeostasis (Burzle et al. 2013; Malik and Willnow 2019; Pizzagalli et al. 2021). For instance, SLC23 is involved in the transport of vitamin C, which protects metabolically active cells from oxidative stress. SLC1A3-mediated clearance of glutamate released by neurons is critical for maintaining appropriate glutamatergic signaling and preventing the accumulation of this amino acid in extracellular toxicity. Besides, the members of SLC5, SLC16, SLC22, and SLC23 subfamilies were also found to transport a diverse set of drugs, toxins, and heavy metals as reported previously (Harris 2000; Xun et al. 2020). Therefore, we speculated that the down-regulation of SLCs in the diseased group may affect the transmembrane transport of antioxidants, neurotransmitters, and harmful substances, contributing to the mortality of the clams.

Additionally, some SLCs may participate in anti-infection immune processes under *Vibrio* infection. He et al. (2022) showed that the expression of SLC1A and SLC8A subfamily members was significantly modulated in oysters infected by *Vibrio alginolyticus*. Chen et al. (2016) suggested that the knockdown of LvSLC15A4 increased the mortality of *Vibrio parahemolyticus*–infected shrimps, revealing a vital immune function in antimicrobial infections. The possible immune-related functions of the down-regulated SLCs identified in this work are warrant of further investigations in the future.

Microbiota disturbances were often fatal and have been recognized as a precursor to death in macroinvertebrates (Wang et al. 2020). We observed a sharp increase of potential pathogenic bacteria (Proteobacteria) and probiotics (Firmicutes) in the hepatopancreas (Fig. 8), indicating that the microbial community may have been disordered after the onset of the disease. Proteobacteria are dominant bacteria in most bivalves, which could compete with host for organic nutrients (Liu et al. 2022). They are revealed to be the most abundant taxa in the gut bacterial community of *Pinna nobilis* in a mass mortality event in the Mediterranean (Lattos et al. 2020). The roles of Proteobacteria in the bivalve disease outbreak warrant further investigations. For Firmicutes, some studies demonstrated the relative proportion of Firmicutes and Bacteroidota (Firmicutes/Bacteroidota ratio) was associated with homeostasis maintaining and energy metabolism, and changes in this ratio can lead to various pathologies (Ma et al. 2022; Stojanov et al. 2020). Therefore, an obvious increase in proportion of Firmicutes in diseased clams may indicate the disruption of homeostasis and influenced energy metabolism, which might contribute to the mortality. In summary, we proposed that the disorder of the microbial community in a clam hepatopancreas may also be a precursor to the summer mortality event, and the change of the microbial community aggravated the occurrence of the mortality event.

Finally, it is notable that our study is limited by the fact that mass mortality occurred naturally in the wild, which lacked biological replicates. Also, we could not determine whether the two batches of clams encountered the same risk of pathogen exposure, or whether the culture conditions of the two ponds, despite that they were spatially adjacent, were indeed similar enough for clams. Since the two ponds were open-water area in a farm, routine operation and maintenance that were not as careful as those in the lab might cause one pond to suffer more risks of pathogen exposure. Other factors might also affect the chemical–physical conditions of the ponds. Although we proposed generally similar conditions of the two ponds due to their spatial proximity and shared water intake, we could not exclude the possibility of some unnoticed factors that may cause varied parameters (e.g., temperatures, salinities) of the water in the two ponds. Lastly, it should be mentioned that the two batches of clams were produced from a genetic breeding project and thus had different genetic backgrounds, which might also contribute to the varied behaviors during mortality event. Therefore, many uncertainties still exist before reaching a comprehensive understanding. On the other hand, as we have revealed, there are evident differences between the clams from diseased and normal groups at various levels (mRNA, protein, microbiota), which we believe to be informative to explore the biological responses/adaptions to stressors leading to summer mass mortality. Some of our major findings, including both changes in the host (e.g., impaired transmembrane transport) and microbiota disturbances in the diseased clams, may shed lights on future investigations on summer mortality.

Conclusion

We analyzed the molecular responses and changes in microbial communities of *M. petechialis* to various stressors leading to mass summer mortality using a variety of omics techniques. The integration of transcriptomic and proteomic analysis revealed that many key metabolic pathways were significantly affected during summer mortality, especially those related to "arginine and proline metabolism" and "tyrosine metabolism." Besides, we revealed that the summer mortality of *M. petechialis* was probably caused by the combined effects of pathogens and environmental factors (high temperatures). Finally, the microbial diversity of hepatopancreas decreased in the diseased group, which reflected microbiota disorder. The present study provided new insights for a better understanding of summer mortality and inferring candidate resistance marker for clam resistance breeding.

Supplementary Information The online version contains supplementary material available at https://doi.org/10.1007/s10126-024-10304-0.

Author Contribution Jing Tian, Hongxia Wang, and Xin Yue performed the experiment. Jing Tian analyzed the data and drafted the manuscript. Pin Huan and Baozhong Liu revised the manuscript.

Baozhong Liu conceived the study and obtained the funding. All authors reviewed and approved the manuscript.

Funding This research was supported by the Strategic Priority Research Program of the Chinese Academy of Sciences (XDA24030304), the Key Research and Development Program of Shandong (2021LZGC029), the earmarked fund for CARS-49, and the Taishan Industrial Leading Talents Project to Shandong Dehe Mingxing Biotechnology Co., Ltd. Chinese Academy of Sciences,XDA2 4030304,XDA24030304.

Data Availability The transcriptome datasets in this study have been submitted to the Sequence Read Archive (SRA) of the National Center for Biotechnology Information with the BioProject accession number PRJNA1025978. The mass spectrometry proteomics data have been deposited to the ProteomeXchange Consortium (http://proteomecentral.proteomexchange.org) via the iProX partner repository with the dataset identifier PXD046074.

Declarations

Ethics Approval The clams are neither an endangered nor protected species. All experiments in this study were conducted according to national and institutional guidelines.

Competing Interests The authors declare no competing interests.

References

Alfaro AC, Nguyen TV, Merien F (2019) The complex interactions of *Ostreid herpesvirus 1*, *Vibrio* bacteria, environment and host factors in mass mortality outbreaks of *Crassostrea gigas*. Rev Aquac 11:1148–1168

Barbosa Solomieu V, Renault T, Travers MA (2015) Mass mortality in bivalves and the intricate case of the Pacific oyster, *Crassostrea gigas*. J Invertebr Pathol 131:2–10

Burdon D, Callaway R, Elliott M, Smith T, Wither A (2014) Mass mortalities in bivalve populations: a review of the edible cockle *Cerastoderma edule* (L.). Estuar Coast Shelf Sci 150:271–280

Burge CA, Griffin FJ, Friedman CS (2006) Mortality and herpesvirus infections of the Pacific oyster *Crassostrea gigas* in Tomales Bay, California, USA. Dis Aquat Org 72:31–43

Burzle M, Suzuki Y, Ackermann D, Miyazaki H, Maeda N, Clemencon B, Burrier R, Hediger MA (2013) The sodium-dependent ascorbic acid transporter family SLC23. Mol Aspects Med 34:436–454

Chen YG, Yuan K, Zhang ZZ, Yuan FH, Weng SP, Yue HT, He JG, Chen YH (2016) Identification and functional characterization of a solute carrier family 15, member 4 gene in *Litopenaeus vannamei*. Dev Comp Immunol 57:57–66

Clegg TA, Morrissey T, Geoghegan F, Martin SW, Lyons K, Ashe S, More SJ (2014) Risk factors associated with increased mortality of farmed Pacific oysters in Ireland during 2011. Prev Vet Med 113:257–267

De Lorgeril J, Lucasson A, Petton B, Toulza E, Montagnani C, Clerissi C, Vidal-Dupiol J, Chaparro C, Galinier R, Escoubas JM, Haffner P, Degremont L, Charriere GM, Lafont M, Delort A, Vergnes A, Chiarello M, Faury N, Rubio T, Leroy MA, Perignon A, Regler D, Morga B, Alunno-Bruscia M, Boudry P, Le Roux F, Destoumieux-Garzomicronn D, Gueguen Y, Mitta G (2018) Immune-suppression by OsHV-1 viral infection causes fatal bacteraemia in Pacific oysters. Nat Commun 9:4215

Degremont L, Ernande B, Bédier E, Boudry P (2007) Summer mortality of hatchery-produced Pacific oyster spat (*Crassostrea gigas*). I. Estimation of genetic parameters for survival and growth. Aquaculture 262:41–53

Edgar RC (2013) UPARSE: highly accurate OTU sequences from microbial amplicon reads. Nat Methods 10:996–998

Fabioux C, Huvet A, Lelong C, Robert R, Pouvreau S, Daniel JY, Minguant C, Le Pennec M (2004) Oyster vasa-like gene as a marker of the germline cell development in *Crassostrea gigas*. Biochem Bioph Res Co 320:592–598

Go J, Deutscher AT, Spiers ZB, Dahle K, Kirkland PD, Jenkins C (2017) Mass mortalities of unknown aetiology in Pacific oysters *Crassostrea gigas* in Port Stephens, New South Wales, Australia. Dis Aquat Org 125:227–242

Grabherr MG, Haas BJ, Yassour M, Levin JZ, Thompson DA, Amit I, Adiconis X, Fan L, Raychowdhury R, Zeng QD, Chen ZH, Mauceli E, Hacohen N, Gnirke A, Rhind N, Di Palma F, Birren BW, Nusbaum C, Lindblad-Toh K, Friedman N, Regev A (2011) Full-length transcriptome assembly from RNA-Seq data without a reference genome. Nat Biotechnol 29:644-U130

Harris ED (2000) Cellular copper transport and metabolism. Annu Rev Nutr 20:291–310

He Y, Li X, Shi C, Li Y, Li Q, Liu S (2022) Transcriptome profiling of the Pacific oyster (*Crassostrea gigas*) suggests distinct host immune strategy in response to *Vibrio alginolyticus* infection. Aquaculture 560:738563

Hine PM, Wesney B, Hay BE (1992) Herpesviruses associated with mortalities among hatchery-reared larval Pacific oysters *Crassostrea-Gigas*. Dis Aquat Org 12:135–142

Ivanina AV, Dickinson GH, Matoo OB, Bagwe R, Dickinson A, Beniash E, Sokolova IM (2013) Interactive effects of elevated temperature and CO2 levels on energy metabolism and biomineralization of marine bivalves *Crassostrea virginica* and *Mercenaria mercenaria*. Comp Biochem Phys A 166:101–111

Jiang FJ, Yue X, Wang HX, Liu BZ (2017) Transcriptome profiles of the clam *Meretrix petechialis* hepatopancreas in response to *Vibrio* infection. Fish Shellfish Immun 62:175–183

Jiang LL, Hong YJ, Xie GS, Zhang JH, Zhang HN, Cai ZW (2021) Comprehensive multi-omics approaches reveal the hepatotoxic mechanism of perfluorohexanoic acid (PFHxA) in mice. Sci Total Environ 790:148160

Lattos A, Giantsis IA, Karagiannis D, Theodorou JA, Michaelidis B (2020) Gut symbiotic microbial communities in the IUCN critically endangered *Pinna nobilis* suffering from mass mortalities, revealed by 16S rRNA amplicon NGS. Pathogens 9:1002

Le Roux F, Gay M, Lambert C, Waechter M, Poubalanne S, Chollet B, Nicolas JL, Berthe F (2002) Comparative analysis of Vibrio splendidus-related strains isolated during *Crassostrea gigas* mortality events. Aquat Living Resour 15:251–258

Li YF, Yang N, Liang X, Yoshida A, Osatomi K, Power D, Batista FM, Yang JL (2018) Elevated seawater temperatures decrease microbial diversity in the gut of *Mytilus coruscus*. Front Physiol 9:839

Li SM, Alfaro AC, Nguyen TV, Young T, Lulijwa R (2020) An integrated omics approach to investigate summer mortality of New Zealand greenshell (TM) mussels. Metabolomics 16:100

Liang BB, Jiang FJ, Zhang SJ, Yue X, Wang HX, Liu BZ (2017) Genetic variation in vibrio resistance in the clam *Meretrix petechialis* under the challenge of *Vibrio parahaemolyticus*. Aquaculture 468:458–463

Liang ZW, Yang LW, Zheng JF, Zuo HL, Weng SP, He JG, Xu XP (2019) A low-density lipoprotein receptor (LDLR) class A domain-containing C-type lectin from *Litopenaeus vannamei* plays opposite roles in antibacterial and antiviral responses. Dev Comp Immunol 92:29–34

Liu BZ, Dong B, Tang BJ, Zhang T, Xiang JJ (2006) Effect of stocking density on growth, settlement and survival of clam larvae, *Meretrix meretrix*. Aquaculture 258:344–349

Liu H, Zha S, Yang Z, Zhang W, Lin Z, Wang S, Bao Y (2022) Acute sulfide exposure induces hemocyte toxicity and microbiota dysbiosis in blood clam *Tegillarca granosa*. Aquat Toxicol 249:106224

Livak KJ, Schmittgen TD (2001) Analysis of relative gene expression data using real-time quantitative PCR and the 2(T) (-Delta Delta C) method. Methods 25:402–408

Lv Z, Qiu L, Wang M, Jia Z, Wang W, Xin L, Liu Z, Wang L, Song L (2018) Comparative study of three C1q domain containing proteins from pacific oyster *Crassostrea gigas*. Dev Comp Immunol 78:42–51

Ma S, Shu X, Wang WX (2022) Multi-omics reveals the regulatory mechanisms of zinc exposure on the intestine-liver axis of golden pompano *Trachinotus ovatus*. Sci Total Environ 816:151497

Magoc T, Salzberg SL (2011) FLASH: fast length adjustment of short reads to improve genome assemblies. Bioinformatics 27:2957–2963

Malik AR, Willnow TE (2019). Excitatory amino acid transporters in physiology and disorders of the central nervous system. Int J Mol Sci, 20.

Monari M, Matozzo V, Foschi J, Cattani O, Serrazanetti GP, Marin MG (2007) Effects of high temperatures on functional responses of haemocytes in the clam *Chamelea gallina*. Fish Shellfish Immun 22:98–114

Nguyen TV, Alfaro AC, Merien F (2019) Omics approaches to investigate host-pathogen interactions in mass mortality outbreaks of *Crassostrea gigas*. Rev Aquac 11:1308–1324

Nie Q, Yue X, Liu BZ (2015) Development of *Vibrio* spp. infection resistance related SNP markers using multiplex SNaPshot genotyping method in the clam *Meretrix meretrix*. Fish Shellfish Immun 43:469–476

Ortega L, Celentano E, Delgado E, Defeo O (2016) Climate change influences on abundance, individual size and body abnormalities in a sandy beach clam. Mar Ecol Prog Ser 545:203–213

Petton B, Pernet F, Robert R, Boudry P (2013) Temperature influence on pathogen transmission and subsequent mortalities in juvenile Pacific oysters *Crassostrea gigas*. Aquacult Env Interac 3:257–273

Pizzagalli MD, Bensimon A, Superti-Furga G (2021) A guide to plasma membrane solute carrier proteins. Febs J 288:2784–2835

Rubiolo JA, Lozano-Leon A, Rodriguez-Souto R, Rodriguez NF, Vieytes MR, Botana LM (2018) The impact of depuration on mussel hepatopancreas bacteriome composition and predicted metagenome. Anton Leeuw Int J G 111:1117–1129

Saco A, Rey-Campos M, Novoa B, Figueras A (2020) Transcriptomic response of mussel gills after a *Vibrio splendidus* infection demonstrates their role in the immune response. Front Immunol 11:615580

Saco A, Panebianco A, Blanco S, Novoa B, Diz AP, Figueras A (2021) Integration of transcriptomics and proteomics improves the characterization of the role of mussel gills in a bacterial waterborne infection. Front Mar Sci 8:735309

Segarra A, Pepin JF, Arzul I, Morga B, Faury N, Renault T (2010) Detection and description of a particular *Ostreid herpesvirus 1* genotype associated with massive mortality outbreaks of Pacific oysters, *Crassostrea gigas*, in France in 2008. Virus Res 153:92–99

Solomieu VB, Renault T, Travers MA (2015) Mass mortality in bivalves and the intricate case of the Pacific oyster, *Crassostrea gigas*. J Invertebr Pathol 131:2–10

Soon TK, Ransangan J (2019) Extrinsic factors and marine bivalve mass mortalities: an overview. J Shellfish Res 38:223–232

Soon TK, Zheng HP (2020) Climate change and bivalve mass mortality in temperate regions. Rev Environ Contam T 251:109–129

Soon TK, Denil DJ, Ransangan J (2016) High mortality and poor growth of green mussels, *Perna viridis*, in high chlorophyll-a environment. Ocean Sci J 51:43–57

Stojanov S, Berlec A, Štrukelj B (2020) The influence of probiotics on the Firmicutes/Bacteroidetes ratio in the treatment of obesity and inflammatory bowel disease. Microorganisms 8:1715

Talmage SC, Gobler CJ (2011) Effects of elevated temperature and carbon dioxide on the growth and survival of larvae and juveniles of three species of Northwest Atlantic bivalves. PLoS ONE 6:e26941

Tan KS, Ransangan J (2015) Factors influencing the toxicity, detoxification and biotransformation of paralytic shellfish toxins. Rev Environ Contam Toxicol 235:1–25

Tian J, Li YJ, Fu HR, Ren LT, He YM, Zhai SY, Yang B, Li Q, Liu NN, Liu SK (2021) Physiological role of CYP17A1-like in cadmium detoxification and its transcriptional regulation in the Pacific oyster, *Crassostrea gigas*. Sci Total Environ 796:149039

Travers MA, Boettcher Miller K, Roque A, Friedman CS (2015) Bacterial diseases in marine bivalves. J Invertebr Pathol 131:11–31

Vaughn CC, Hoellein TJ (2018) Bivalve impacts in freshwater and marine ecosystems. Annu Rev Ecol Evol S 49:183–208

Vezzulli L, Previati M, Pruzzo C, Marchese A, Bourne DG, Cerrano C, Consortium V (2010) *Vibrio* infections triggering mass mortality events in a warming Mediterranean Sea. Environ Microbiol 12:2007–2019

Villalba A, Carballal MJ, Lopez C, Cabada A, Corral L, Azevedo C (1999) Branchial rickettsia-like infection associated with clam *Venerupis rhomboides* mortality. Dis Aquat Org 36:53–60

Wang H, Yue X, Yu J, Wang R, Teng S, Fang J, Liu B (2020) Microbial community changes in the digestive tract of the clam *Meretrix petechialis* in response to *Vibrio parahaemolyticus* challenge. Journal of Oceanology and Limnology 39:329–339

Xiao H, Ford SE, Yang HS, Zhang GF, Zhang FS, Guo XM (2005) Studies on mass summer mortality of cultured zhikong scallops (*Chlamys farreri* Jones et Preston) in China. Aquaculture 250:602–615

Xun XG, Cheng J, Wang J, Li YP, Li X, Li ML, Lou JR, Kong YF, Bao ZM, Hu XL (2020) Solute carriers in scallop genome: gene expansion and expression regulation after exposure to toxic dinoflagellate. Chemosphere 241:124968

Yang B, Zhai SY, Li X, Tian J, Li Q, Shan HW, Liu SK (2021) Identification of *Vibrio alginolyticus* as a causative pathogen associated with mass summer mortality of the Pacific oyster (*Crassostrea gigas*) in China. Aquaculture 535:736363

Young MD, Wakefield MJ, Smyth GK, Oshlack A (2010) Gene ontology analysis for RNA-seq: accounting for selection bias. Genome Biol 11:R14

Yue X, Liu BZ, Xiang JH, Jia JT (2010) Identification and characterization of the pathogenic effect of a *Vibrio parahaemolyticus*-related bacterium isolated from clam *Meretrix meretrix* with mass mortality. J Invertebr Pathol 103:109–115

Yue X, Huan P, Hu YH, Liu BZ (2018) Integrated transcriptomic and proteomic analyses reveal potential mechanisms linking thermal stress and depressed disease resistance in the turbot *Scophthalmus maximus*. Sci Rep-Uk 8:1896

Zannella C, Mosca F, Mariani F, Franci G, Folliero V, Galdiero M, Tiscar PG, Galdiero M (2017) Microbial diseases of bivalve mollusks: infections, immunology and antimicrobial defense. Mar Drugs 15:182

Zhang SJ, Yue X, Jiang FJ, Wang HX, Liu BZ (2017) Identification of an MITF gene and its polymorphisms associated with the *Vibrio* resistance trait in the clam *Meretrix petechialis*. Fish Shellfish Immun 68:466–473

Zhang S, Yue X, Yu J, Wang H, Liu B (2019) MITF regulates downstream genes in response to *Vibrio parahaemolyticus* infection in the clam *Meretrix Petechialis*. Front Immunol 10:1547

Zou LH, Liu BZ (2016) The polymorphisms of a MIF gene and their association with *Vibrio* resistance in the clam *Meretrix meretrix*. Dev Comp Immunol 62:116–126

Authors and Affiliations

Jing Tian[1,4] · Hongxia Wang[1,2] · Pin Huan[1,2,3] · Xin Yue[1,2] · Baozhong Liu[1,2,3,4]

✉ Baozhong Liu
bzliu@qdio.ac.cn

Jing Tian
tianjing@qdio.ac.cn

Hongxia Wang
hxwang@qdio.ac.cn

Pin Huan
huanpin@qdio.ac.cn

Xin Yue
yuexin@qdio.ac.cn

[1] CAS and Shandong Province Key Laboratory of Experimental Marine Biology, Institute of Oceanology, Chinese Academy of Sciences, Qingdao 266071, China

[2] Laboratory for Marine Biology and Biotechnology, Qingdao Marine Science and Technology Center, Qingdao 266000, China

[3] Key Laboratory of Breeding Biotechnology and Sustainable Aquaculture, Chinese Academy of Sciences, Qingdao 266071, China

[4] University of Chinese Academy of Sciences, Beijing 100049, China